Tutorial

Patryk Mlyniuk, Ewa Maczynska-Walkowiak, Jagoda Rzeszewska-Zamiara, Ireneusz Grulkowski* and Bartlomiej J. Kaluzny

Probing biomechanical properties of the cornea with air-puff-based techniques – an overview

https://doi.org/10.1515/aot-2021-0042
Received September 1, 2021; accepted October 29, 2021; published online November 22, 2021

Abstract: The cornea is a part of the anterior segment of the eye that plays an essential optical role in refracting the light rays on the retina. Cornea also preserves the shape of an eyeball and constitutes a mechanical barrier, protecting the eye against the factors of the external environment. The structure of the cornea influences its biomechanical properties and ensures appropriate mechanical load transfer (that depends on the external environment and the intraocular pressure) while maintaining its shape (to a certain extent) and its transparency. The assessment of the corneal biomechanics is important in clinical ophthalmology, e.g. in the diagnosis of ectatic corneal diseases, for precise planning of the refractive surgery, and in accurate determination of the intraocular pressure. A standard technique to determine corneal biomechanics requires the application of well-defined mechanical stimulus (e.g. air puff) and performing simultaneous imaging of the response of the tissue to the stimulus. A number of methods to assess the biomechanical properties of the cornea have been developed, including ultrasound, magnetic resonance imaging, and optical methods as visualization modalities. Commercially available methods include the ocular response analyzer (ORA) and corneal visualization scheimpflug technology (Corvis ST). Currently advanced research is conducted using optical coherence tomography (OCT). The extension of OCT called optical coherence elastography (OCE) possesses high clinical potential due to the imaging speed, noncontact character, and high resolution of images.

Keywords: air puff OCT; corneal elastography; keratoconus; optical coherence elastography; viscoelasticity.

1 Introduction

The cornea is a transparent, outermost part of the eye. Not only the cornea constitutes an essential element of the optical system of the eye, but also it forms a mechanical barrier against the factors of the external environment to protect the soft inner part of the eye. Due to its transparency, curvature, and anterior surface smoothness, the cornea resembles a watch crystal. The cornea transmits over 80% of visible light and participates in its refraction (40–44 D), along with the tear film and the intraocular lens (20 D), enabling light focusing on the retina and the perception of visual stimuli [1–4].

Due to its location, the cornea is exposed to various external factors (including variations in atmospheric pressure, eyelid movements, eye rubbing, dehydration, etc.) and diurnal intraocular pressure (IOP) fluctuations at the same time (internal and external sources of stress). Hence, corneal biomechanical properties manifested by elasticity, tensile strength, and ability to distribution of the stress are crucial for maintaining the proper shape (geometry) and, therefore, appropriate refraction and stable visual perception (Figure 1) [1–7].

The biomechanical properties of the cornea arise from biochemical and physical structure of the corneal tissue [8]. The mechanical properties are influenced by the composition and organization of fibers, cells, and ground substance [8]. The strength and elasticity of the cornea depend on collagen and elastin fibers [7, 8]. In turn, the viscosity depends on noncovalent rearrangements of the extracellular matrix (ECM) [7, 8], which transmits external mechanical loads to the resident cells, leading to their spreading and migration [9].

***Corresponding author: Ireneusz Grulkowski**, Institute of Physics, Faculty of Physics, Astronomy and Informatics, Nicolaus Copernicus University in Toruń, ul. Grudziądzka 5, 87-100 Toruń, Poland, E-mail: igrulkowski@fizyka.umk.pl. https://orcid.org/0000-0001-7688-1826
Patryk Mlyniuk, Jagoda Rzeszewska-Zamiara and Bartlomiej J. Kaluzny, Department of Ophthalmology, Division of Ophthalmology and Optometry, Collegium Medicum, Nicolaus Copernicus University in Toruń, ul. Ujejskiego 75, 85-168 Bydgoszcz, Poland
Ewa Maczynska-Walkowiak, Institute of Physics, Faculty of Physics, Astronomy and Informatics, Nicolaus Copernicus University in Toruń, ul. Grudziądzka 5, 87-100 Toruń, Poland

The assessment of the biomechanical properties of the cornea has increasing clinical applications. The biomechanics of the cornea and its thickness are important in the measurement of the intraocular pressure (IOP) as well as in a more effective diagnosis and treatment of glaucoma. Most frequently, in the case of IOP measurement, correction tables are used taking into account the impact of corneal thickness, ignoring its dynamic properties [4, 5, 8, 10, 11]. Information on the viscoelastic properties of the cornea, in addition to its topography, is extremely important in the diagnosis, management and evaluation of the progression of ectatic corneal diseases such as keratoconus (KC), pellucid marginal degeneration (PMD), and megalocornea. This makes it possible to evaluate changes in tissue stiffness, which is reduced in the case of ectatic corneal diseases, as well as its response to external stress [4, 5, 8, 10–12]. In addition, the assessment of the corneal biomechanics is useful for planning the refractive surgery and detecting contraindications to increase predictability of surgical procedure and at the same time to reduce the risk of iatrogenic ectasia [4, 8, 10, 12, 13].

In this paper, we present different aspects of corneal biomechanics and the role of biomechanics in ensuring proper eye functions. The tutorial focuses on the methods of assessing corneal biomechanics, with particular emphasis on commercialized optical techniques and their clinical application, as well as their alternative noncommercial methods mainly based on optical coherence tomography (OCT) under an air stream excitation.

2 Corneal structure and its impact on biomechanics

The cornea is a complex structure that ensures the integrity and proper functioning of the entire optical system of the eye. The corneal diameter ranges from 9 to 11 mm vertically and 11–12 mm horizontally. The average radii of curvature of the anterior and posterior surfaces of the cornea are 7.79 mm and 6.53 mm, respectively [14]. The cornea consists of six layers: epithelium, Bowman's layer, stroma, a pre-Descemet's membrane, Descemet's membrane and endothelium, and its average central thickness is 551–565 µm [1–3]. Each layer has an individual configuration of structure with differences in the type, orientation and density of collagens, elastins, fibronectins, laminins, and proteoglycans, which form strong fibers and networks as a type of staging for tissue [3]. The Bowman's layer and stroma play the most important role in corneal biomechanics [3].

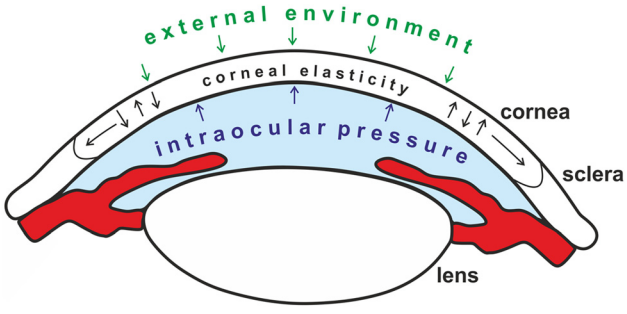

Figure 1: Scheme of the general relation between the external environment, intraocular pressure, and elasticity of the cornea.

The epithelium is the cornea's outermost layer and, therefore, the most exposed to external factors. It takes about 10% of its central thickness and is built of easily regenerated, multilayered, non-keratinized cells [1, 2, 7]. In general, the epithelium as a pure cell layer is supposed to have no influence on corneal rigidity. Elsheikh and et al. testing human donor eyes confirmed insignificant epithelium participation in corneal stiffness compared to stroma [7]. Nevertheless, it is important to remember that the corneal epithelium is easily deformable and its anteriar surface is used as the reference in the majority of techniques of measuring biomechanical properties [8].

The Bowman's layer and the stroma take together 90% of the corneal thickness and are the main collagenous layers of the cornea [1–3, 8]. Therefore, those layers contribute most to the cornea's tensile strength [8]. The diameter and orientation of collagen fibrils determines corneal transparency and has an impact on visual acuity [7]. The Bowman's layer is an acellular structure composed of randomly-oriented collagen fibrils [1–3, 7] and it is considered to be essential for the corneal biomechanics after laser ablative surgery [3, 4, 7].

In the stroma, the collagen (mainly type I collagen fibrils) is laid down within around 200 lamellae, orthogonally oriented in the center and circumferentially in the periphery of the layer [3, 12, 13, 15]. The orthogonal arrangement of the fibers ensures the correct shape of the cornea and the highest visual acuity [7]. Nonlinear optical microscopy technique found more extensive intralamellar branching and steeper angles of the collagen fibers in the anterior than in the posterior cornea, which is due to the increased packing of these fibers and their highly interwoven structure in the central cornea. This finding correlates with an increased shear stress in the anterior cornea compared to the posterior cornea in response to the applied force due to the greater anterior elastic moduli in its central and paracentral regions [7, 12, 15]. In the peripheral regions, the posterior elastic modulus is higher than the

anterior elastic modulus [12]. In turn, the second harmonic generation imaging microscopy found a gradual increase in the width of collagen lamellae from the anterior to posterior stroma. In addition, the arrangement of the collagen bundles in the posterior corneal lamellae is more regular [12].

An important corneal constituent for the biomechanics of the corneal stroma is the extracellular matrix (ECM) consisting of glycosaminoglycans (GAGs) and proteoglycans (PGs). GAGs and PGs play an essential role in the assembly of the ECM and its transparency. GAGs are highly polar molecules that affect the viscosity of a tissue by increasing water the adhesion of water molecules [3, 7, 12, 15, 16]. GAGs are compulsory to sulfate PG core proteins, namely keratan sulfate (KS), chondroitin sulfate (CS)/dermatan sulfate (DS), heparan sulfate, and hyaluronan, but have almost no influence on nucleation or growth due to only electrostatic impediment with collagen [7, 12]. KS-PGs control the diameter of collagen fibrils and stabilize them over a short range, while DS-PGs modify lamellar adhesion and determine the interfibrillar spacing [7, 12]. In turn, the role of CS-PGs is to stabilize several fibrils as far as the lamellae, and its deficiency potentially weakens the cornea and leads to corneal ectasia [7, 12].

The energy dissipation during the deformation of the cornea under load is closely related to the viscous sliding of the fibrils and lamellae in PGs, and the rearrangement of water molecules [4]. The amount of oxygen has a major influence on proportions of GAGs and PGs, especially conditions of O_2 deficiency determine production of keratan sulfate that can describe why KS lead in the posterior stroma [7].

The number of acidic GAGs corresponds directly to the degree of collagen fibers organization in the human corneal stroma [7]. It has been proposed that particularly deglycosylated small leucine-rich repeat proteoglycan core proteins may modify the collagen fibrillogenesis and could be instrumental in some corneal ectatic disorders. In KC, PMD and macular corneal dystrophy the quantity of highly sulfated KS-PGs is decreased or gone, respectively [7].

Pre-Descemet's membrane or Dua's layer (pDM) and is very similar to the adjacent stromal structure. Differences include a higher density of lamellae and a greater spacing between collagen fibrils, indicating differences in proteoglycans [3].

The DM , 3–5 μm thick, is an acellular fibrous layer formed by the hexagonal lattice of collagen [3]. The DM fibers adhere to the posterior surface of the stroma and are able to reflect changes in stromal shape although collagen stromal fibers are not an extension in DM [12]. The DM is the basement membrane for endothelial cells [12].

The endothelium layer is a mitochondria-rich cell monolayer and it is approximately 5 μm thick [1–3, 12]. The corneal endothelium plays a crucial role in maintaining the transparency of the cornea, and its proper hydration, which indirectly influences the stiffness of the cornea [7, 12]. As tissue hydration increases, its elastic modulus decreases, which is associated with changes in the collagen attachment with PGs and/or GAGs based on their ionic interactions [7]. Endothelial cells allow for diffusion of nutrients to the other corneal layers, as they are avascular [1, 2].

3 Corneal biomechanics

The cornea, like most of the soft tissues, is a viscoelastic material, which means that its mechanical properties are time-dependent. The stress–strain relationship is nonlinear (J-shape) and can be divided into two characteristic parts reflecting changes in the collagen organization under increasing stress (Figure 2). Lower region of the curve reflects slow, low-strain response of stromal matrix during which collagen fibrils are uncrimping and reorienting towards stress direction. At low strain, corneal tissue shows mainly viscous property, while at large strain values, the elastic response governed by stretching of the fibrils is dominant [17]. For this reason, it is challenging to assess the corneal biomechanics correctly, and there are many approaches to do it, from basic engineering mechanical characterization to advance elastography methods.

Combination of elastic and viscous behavior makes a cornea a perfect mechanotransducer of the stress [17]. For viscoelastic materials, after removing the force, the material's return to original shape is delayed. The difference in loading and unloading paths, manifested by hysteresis loop, is related to loss of energy inside the tissue (Figure 2) [3–5, 7, 8, 18, 19]. The ability to dissipate energy is an important defense mechanism that counteracts premature tissue impairment and permanent change in corneal shape with time [5, 7, 9, 17]. Due to the fact that the cornea is a viscous and elastic tissue, its mechanical and hydrodynamic properties in the stress–strain relation can be described by the combined Hookean and Newtonian method [20].

The engineering gold standard used to determine the mechanical properties of various materials is Young's modulus E, defined as the ratio of stress ($\Delta\sigma$) to strain ($\Delta\varepsilon$),

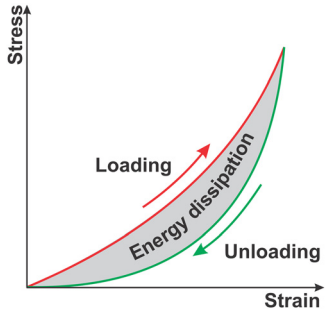

Figure 2: Stress–strain relationship for viscoelastic materials. Red and green curves represent the behavior of viscoelastic materials during loading and unloading conditions, respectively. The difference in loading (deformation) and unloading (recovery) paths, manifested by hysteresis loop, is related to energy dissipation during deformation/recovery process.

which describes the material response to axial stress [6, 7, 17, 18, 21–23]:

$$E = \frac{\Delta\sigma}{\Delta\epsilon}. \tag{1}$$

The stress and the strain are expressed by [6, 17, 23]:

$$\Delta\sigma = \frac{F}{A}, \tag{2}$$

$$\Delta\epsilon = \frac{\Delta L}{L_0}, \tag{3}$$

where F is applied force (acting perpendicularly to the cross-section of the sample), A is the cross-sectional area of the sample, L_0 is an original length of the sample, and ΔL is a change in sample length (extension).

According to Eqs. (1)–(3), $\sigma = E\epsilon$, where Young's modulus is a proportionality factor (material's constant) that relates to stress and strain, and it is a way to expresses how stiff the material is. The higher the E, the more rigid the tissue is and the greater its resistance to the applied force [5, 8, 17]. Young's modulus termed as modulus of elasticity can be applied only to linear region of stress–strain curve ($\sigma \infty \epsilon$, Hooke's law). Therefore, due to of non-linear nature of viscoelastic materials, E can be calculated only for very low values of strain [6, 7]. Nevertheless, depending on the method used, the E values for the cornea may vary by several orders of magnitude, which is a significant problem in reliably of establishing its true value [7, 24]. Another way to describe elastic properties of the cornea during extension are more general methods based on secant and/or tangent modulus calculation [6].

In general, elasticity is a material ability to resist its deformation. Apart from elongation (extension) of the tissue employed to obtain Young modulus, is possible to assess the corneal elasticity by measuring the resistance of the tissue due to the effect of shear deformation. In this case, the formula takes the form:

$$\sigma = G\gamma, \tag{4}$$

where G is a shear modulus (elastic modulus, material's constant) and γ is shear strain [21].

The shear modulus describes the material response to a shear stress, i.e. the deformation of a tissue while applying a force parallel to one of its surfaces, when the opposite surface experiences an opposite force [6, 21, 22, 25–28].

There is no single parameter that can fully describe the elastic behavior of the cornea since it does not have a simple mechanical nature. Therefore, Young's and shear modulus are equivalent in measuring tissue response to one-dimensional stress [19]. The shear modulus can be calculated using the Young's modulus and conversely:

$$G = \frac{E}{2(1+\nu)}, \tag{5}$$

$$E = 2G(1+\nu), \tag{6}$$

where G is shear modulus, E is Young's modulus, and ν is Poisson's Ratio [23, 26].

4 Elastographic methods of corneal biomechanics assessment

The diseases may change local stiffness of the tissue. Therefore, physicians made a diagnostic tool from their hands to find and assess the potential tumors. Palpation techniques have allowed to 'touch the disease' and have become the foundation for imaging biomechanical properties through the development of elastography. Elastography is a relatively new, dynamically growing research area that incorporates several approaches to image mechanical properties of the various tissues. Regardless of the method chosen, the main idea is to stimulate the tissue with a force, measure the displacements distribution inside the material under loading conditions and, based on it, assess the mechanical properties of the tissue [3, 7, 8, 10, 29]. Figure 3 presents a summary of various approaches used in corneal elastography.

The mechanical excitation can be induced in many ways. The load can be applied in contact (via glass plate [30], gonioscopy lens [31]) or noncontact manner (air stream [11, 32, 33], airborne ultrasound [34], sounds [35]). On the other hand, the applied stimulus can be divided according to type of loading (static/quasi-static or dynamic), pattern (impulse, constant), direction of the applied force, as well

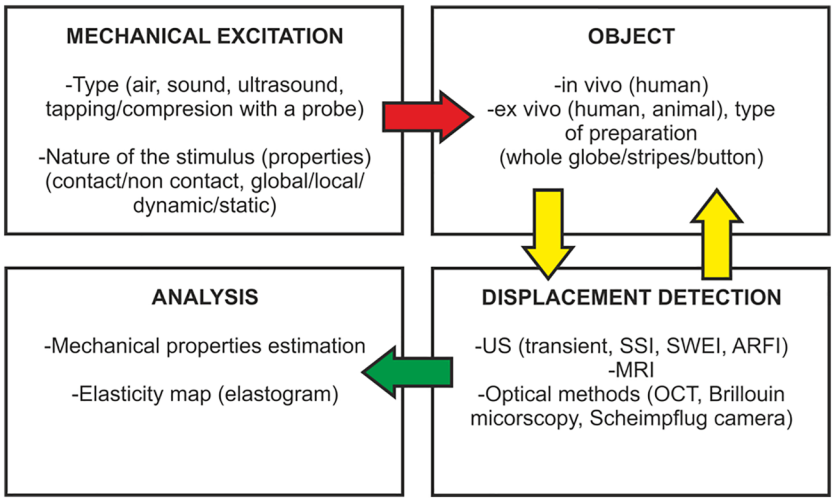

Figure 3: A short summary of various approaches used in corneal elastography. In order to induce tissue perturbation, a proper type of mechanical loading is applied (red arrow). Next, the response of the tissue due to excitation is imaging and recorded (yellow arrows). At the last stage, tissue displacement is analyzed and may be transformed into mechanical properties (green arrow).

as the scale of observed deformation (macro-/micro-/nanoscopic, global/local) [11, 30–33, 35–38]). In turn, the tests can be performed *in vivo* [33, 37, 38], *in vitro* [39] or *ex vivo* [31, 40] in human and model eyes of animals (pigs, cattle, rabbits, and mice) [11, 41–43]. In *ex vivo* methods, i.e. outside the living organism, tissue sections, strips, buttons as well as the entire eye globes are examined, which allows the tissues to be subjected to various loading patterns as opposed to *in vivo* methods [10, 16]. Tissue preparation destroys corneal structure and spherical geometry, as well as introduces additional boundary stress, which influences mechanical tissue characterization [10, 16, 27]. Additionally, the orientation of fibers may be disturbed by cutting and climbing tissue to the machine before measurement [10, 16, 27, 28]. Moreover, *ex vivo* measurement involve the risk of dehydration, swelling, and loss of clarity after death, which also may influence on outcomes [16, 28]. Therefore, the need of overcoming these limitations and developing methods to measure corneal biomechanics *in vivo*, paved the way to adopt and/or develop more advanced strategies of elastography, which are based on different assumptions.

Apart from applying well-defined stimulus, visualization of the tissue reaction is crucial in the procedure of the assessment of corneal biomechanics. The tissue deformation can be determined indirectly or imaged directly. The imaging modalities used to measure the corneal displacement during stimulation include ultrasound (ultrasound elastography – UE), magnetic resonance imaging – MRI (magnetic resonance elastography – MRE) as well as a wide group of optical methods [24, 31, 33, 34, 36, 40, 41, 44–46]. The visualization strategy enables to acquire images of the dynamics of the cornea in a form of consecutive line scans (axial scans), cross-sectional images, or volumetric (three-dimensional) data.

The first elastography instruments used ultrasound (US) of very high frequency (≥50 MHz) as a method of visualizing the displacement of the tissue under compression [34, 45, 46]. These methods are based on ultrasound elastography [45], high-frequency ultrasonographic analysis of corneal changes [45], supersonic shear-wave imaging [4] and ocular pulse elastography (OPE) [46]. The OPE technique allows for a precise quantitative assessment of the corneal deformation per eye impulse using high-frequency ultrasonic spot tracking [46]. The disadvantages of standard UE are the contact nature of the examination and the low resolution of the images, from which precise data describing the biomechanics of the examined tissue should be obtained.

The MRE is a highly sensitive MRI method with phase contrast. It allows to visualize the microscopic displacements and mechanical properties of the examined tissue [41, 44, 47]. Elastograms obtained from the MRI images may have half the resolution of the native MRI images, which ranges from 50 μm to 10 mm, but most often have 20–30% of the MRI resolution [44]. The examination consists of introducing mechanical vibrations of a known frequency (50–500 Hz) and encoding the resulting tissue movement using the MRI technique with a synchronous gradient field. This method has several advantages like a large penetration depth and a wide field of view. However, due to its low spatial resolution, long imaging time and high cost, the MRE is not suitable for clinical ophthalmic applications [41, 44].

The optical methods used for the evaluation of biomechanical properties include Brillouin optical microscopy [48], photography [49, 50], holography [51, 52], and optical

coherence tomography (OCT) [4, 8, 11, 33, 36–38, 42, 43, 53–64], the implementation of which became a breakthrough in the development of eye elastography. In contrast to UE and MRE, the optical coherence elastography (OCE) methods enable imaging the tissue with micrometer resolution, therefore bringing opportunity to detect diseases at the very early stage. Moreover, the devices based on the OCT are characterized by high sensitivity and high speed of scanning the examined tissue. In the case of OCE, multiple approaches to stimulate the tissue can be used, and the most popular techniques involve an air stream or ultrasound [24, 31, 33, 36, 40]. The technique uses air-coupled ultrasound to stimulate the mechanical tissue with precise spatial and temporal shaping (acoustic microtapping, AμT) [34]. The applied four-dimensional OCT (3-D + time) enables high-resolution and quantitative imaging of dynamic response of the examined tissue [34]. The shear wave imaging (SWI-OCT) can also be used to quantify the viscoelastic properties of the cornea [36].

From the clinical point of view, the most attractive methods are those in which the stimulation is realized in a non-contact mode. A widely recognized approach is to use an air stream to stimulate the cornea. Such a strategy can be found in two commercial devices for measuring corneal biomechanics, i.e. ocular response analyzer and corneal visualization scheimpflug technology [4, 8, 10, 41]. In noncommercial studies, the air-puff stimulation has been coupled primarily with OCT systems. Combined advantages of noncontact stimulation and OCT imaging allow gaining new knowledge on cornea behavior thus opening gates for wide clinical application in the future. These methods will be described below.

4.1 Ocular Response Analyzer

The ocular response analyzer (ORA) is a noninvasive tonometer manufactured by Reichert ophthalmic instruments (Buffalo, New York, USA) in 2005 [4, 5, 8, 45, 65]. *In vivo*, it allows for detection of the reaction of the cornea for 25 ms of air puff stimulus [65], directed through the air tube into a central 3–6 mm apical corneal area, using a fully automated alignment system positions [4, 65]. The device uses an infrared emitter, an electro-optical infrared (IR) detection system, a solenoid driven air pump and a pressure sensor inside the plenum chamber [45, 65]. During the measurement, the central part of cornea is illuminated with infrared light and the detector records the intensity of the light reflected from the cornea [45]. When properly aligned with the apex of the cornea, the stream of the air begins to flatten the initially convex cornea, and as it becomes flat, the first applanation (P_1) occurs (Figure 4A). Then the cornea deforms inward to become a slight concavity and, while returning to its convexity, the second applanation (P_2) occurs when the surface is flat. At the moment of obtaining two flattening states (P_1 and P_2), the intensity of the reflected light is maximal, therefore the signal is very high (peak) [4, 5, 8, 45, 66, 67]. The device simultaneously records the force of the air stimulus and measures the reflection of the light, which allows to determine at which air pressure the applanations are achieved. Due to the viscoelastic properties of the cornea, the deformation and return to equilibrium are different, so that the two applanations reach different pressures [4, 5, 8, 45, 66, 67]. It should be noted that ORA does not compensate for the whole eye movement caused by the air stream, which affects the results obtained.

According to the manufacturer, the ORA enables to assess the corneal hysteresis [8, 45]. The corneal hysteresis (CH) is a parameter expressing the tissue response to the air stream [8, 10, 45, 65, 67]. This parameter is considered as the rate of the corneal viscosity, and is defined as the difference between the first (P_1) and the second (P_2) applanation (Figure 4A) [4, 5, 8, 13, 19, 45, 65–68]:

$$CH = P_1 - P_2, \tag{7}$$

however, a hysteresis loop is necessary for the detailed evaluation of energy dissipation, as it determines the level of the energy absorption and dissipation after corneal deformation, and consequently its return to the equilibrium [8–10, 45, 65, 67]. The ORA device does not provide information on the energy lost in Joules (J) during the stress–strain cycle [5]. It allows to observe the viscoelastic properties manifested only by differences in the behavior of the tissue when the strength of the stimulus increases and when it subsides, which is defined by the manufacturer as CH, which is a manifestation of the viscoelastic nature of the cornea, but deviates from the physical definition of the hysteresis loop [5, 8–10, 45, 65, 67]. The CH is positively correlated with the central corneal thickness (CCT) [5, 8], but is not related to the central corneal radius of curvature [67, 68].

In the normal eyes, the CH ranges from 9.3 ± 1.4 to 11.43 ± 1.52 mmHg [10, 45]. The relationship between age and changes in CH is not fully understood [8]. El Massry et al. found that the CH significantly decreases with age, which is associated with an increase in corneal stiffness with a simultaneous decrease in its viscosity [3, 45, 69]. In turn, other studies show the opposite correlation or no dependence [8]. In the case of KC, Fuchs corneal dystrophy (FCD) and other disease with progressive changes in the CCT, the CH is lower [5, 70], but corneal crosslinking (CXL) treatment will increase this parameter [3, 19, 45]. The CH is an important constituent in assessing the progression of

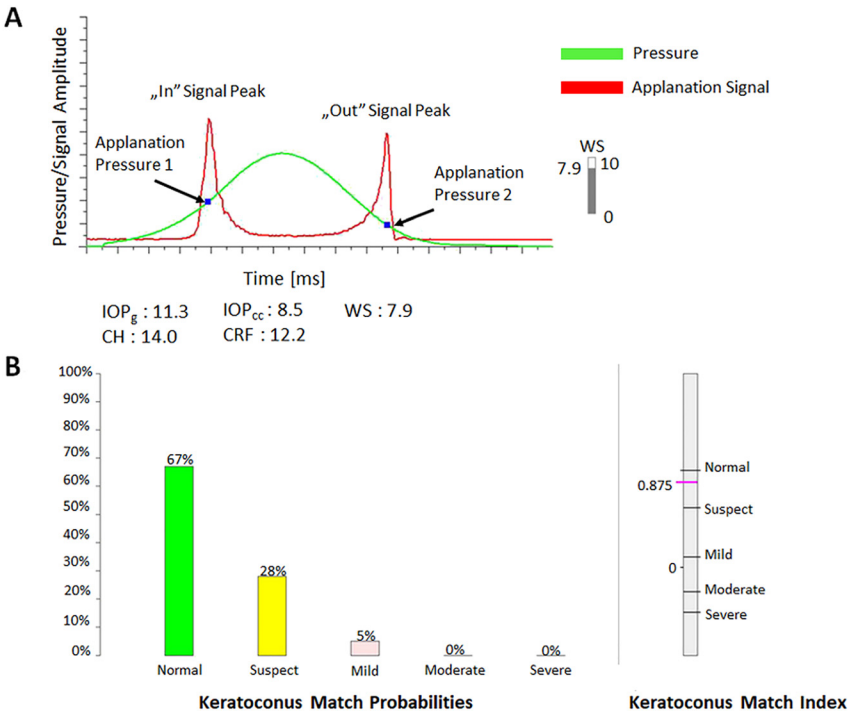

Figure 4: The ORA score in the normal eye. A. The graph shows the pressure/signal amplitude during the measurement and the amount of light reflected by the cornea at the same time. Basic results from the device: Goldmann-correlated IOP (IOPg), the corneal-compensated IOP (IOPcc), the corneal hysteresis (CH), the corneal resistance factor (CRF), and the waveform score (WS) – the measurement quality parameter. B. The graphs show the keratoconus match probabilities and keratoconus match index (adopted from the ORA with permission from the Optotech Medical Poland).

glaucoma [45, 65, 66, 71, 72]. Medeiros et al. [71] found that lower CH is associated with faster loss of visual fields. Moreover, this parameter significantly decreases after corneal refractive surgery [5, 45, 69], especially after LASIK [45], as the changes in the viscoelastic properties of the cornea are greater [73].

The second important parameter obtained from the ORA is the corneal resistance factor (CRF) [5, 7, 8, 45, 66]. The CRF is considered as the rate of the overall resistance of the cornea to the deformation [13], which is relevantly related to the elastic properties of the cornea and the CCT [5, 8, 45, 66] but is not associated with central corneal radius of curvature [67, 68]. The CRF can be obtained from the following formula [5, 8, 19, 45, 65, 66, 68]:

$$CRF = P_1 - k \cdot P_2, \tag{8}$$

where k is constant value defined by an empirical analysis of the relationship between the first and the second applanation, and the CCT [5, 45, 65]. The manufacturer stated that k has the value of 0.7 [66]. Some authors have also developed a modified formula:

$$CRF = k_1 [P_1 - 0.7 \cdot P_2] + k_2, \tag{9}$$

where k_1 and k_2 are the constants to maximize correlation with the CCT [8, 67].

In the normal eyes, the CRF calculated from the original formula ranges from 9.2 ± 1.4 mmHg to 11.9 ± 1.5 mmHg [10, 45]. El Massry et al. [69] found that the CRF significantly decreases with age. Moreover, the CRF significantly decreases after corneal refractive surgery [5, 69], as in the case of the CH [45, 73]. In addition, Hashemi et al. [74] found that the CRF is an indicator with very high sensitivity and specificity for the detection of early KC.

Table 1 summarizes the values for the CH and CRF for normal eyes as well as in various pathological conditions and as a result of the applied treatment.

The newer ORA software enables evaluation of the corneal ectasia with two specific parameters [75]: the keratoconus match probability (KMP) and keratoconus match index (KMI) (Figure 4B). The KMP is an index that indicates the probability of KC as a percentage, classifying the cornea as normal, suspicious, and with mild, moderate or severe KC [75]. The KMI is related to similarity of the waveform of the examined eyes in relation to the mean waveform scores of KC in the database by calculating the neural network of seven waveform scores [75]. The KMI is approximately 1 for the cornea classified as normal, whereas the cornea with KC will achieve KMI around 0 [75].

Another parameter obtained from the ORA is the corneal constant factor (CCF), which is IOP-independent

Table 1: The CH and CRF values for normal eyes and their changes in various conditions.

		CH	CRF
Mean value (mmHg)		9.3 ± 1.4 to 11.43 ± 1.52	9.2 ± 1.4 to 11.9 ± 1.5
Correlation with the eye parameters	CCT	Positive	Positive
	Curvature of the cornea	–	–
	Refractive error	Negative in high myopia	–
Dependence on age		↓	↓
The effect of	Keratoconus	↓	↓
	CXL	↑	↑
	Laser vision correction	↓	↓

and increases with thicker CCT and decreases with aging [5, 8]. The CCF was proposed by Reichert and can be obtained from the formula [8]:

$$CCF = P_1 - 0.79 \cdot P_2. \tag{10}$$

The ORA provides also the IOP measurement: Goldmann intraocular pressure (IOP_g) and corneal-compensated intraocular pressure (IOP_{cc}). The IOP_g is calculated as the average value of the first (P_1) and the second (P_2) applanation [8, 10]:

$$IOP_g = \frac{P_1 + P_2}{2}. \tag{11}$$

Unlike standard tonometers, the IOP_{cc} is correlated with CH and is described by the formula [8, 10]:

$$IOP_{cc} = P_1 - 0.43 \cdot P_2. \tag{12}$$

Additionally, the new ORA software provides 37 parameters that analyze the corneal deformation signal waveform in detail, but these are not widely used in clinical practice [76–78]. The device also offers the possibility of creating 15 candidate variables from the obtained data for characterization the temporal, applanation signal intensity and pressure features of the corneal response [79]. Advanced algorithms, such as machine learning, including deep learning, in which discriminative and generative models are used, can also be used for waveform analysis. One of the approaches to deep learning is variational autoencoders (VAEs) but their usefulness in ophthalmology has not yet been assessed [78].

4.2 Corneal Visualization Scheimpflug Technology

The corneal visualization scheimpflug technology (Corvis ST) is a non-contact tonometer, pachymeter and device for biomechanical analysis of the cornea introduced by Oculus (Wetzlar, Germany) in 2011 [4, 45, 80]. In relation to the ORA, the Corvis ST takes images of the anterior segment at a rate of 4330 frames per second [19, 45, 80, 81] and collect approximately 140 cross-sectional images over a period of 33 ms to record the deformation and recovery of the cornea with an ultrahigh-speed (UHS) Scheimpflug camera [4, 81–84]. Each image has 576 measuring points (80,640 points per examination) over 8.5 mm (0.3 in), which ensures high-quality images. Blue LED light beam of a wavelength of 455 nm is used for measurement. The beam illuminates the area from the front to the back surface of the cornea. Light scattering results in glowing of the illuminated area. The camera records this effect at an angle of 45° to the pupil. In order to achieve the same sharpness over the entire area, and at the same time sharp cross-sectional images of the cornea, the photosensitive area is also positioned at a 45° angle to the lens (Scheimpflug principle) [81, 85]. Moreover, the Corvis ST ensures a constant maximal peak pressure for the air puff in each examination [4].

The Corvis ST deforms the cornea inward and outward using an air stream of a pressure of 25 kPa, and during the measurement a double applanation occurs. This measurement is made in a transverse section and passes through the apex of the cornea [45, 80, 81, 84].

In addition, the next-generation of Corvis ST analyses whole eye motion by analyzing the displacement of periphery of the cornea during air-puff stimulation, providing a more reliable assessment of the dynamic corneal response (DCR) [4, 56].

The Corvis ST allows to export images for own analysis. The created algorithms enable numerical analysis of the local distribution of the curvature of the corneal profile as a result of dynamic deformation, as well as the description of new dynamic parameters of the cornea [86]. The ongoing studies aim at detecting the outer corneal edge. One of the proposed algorithms is based on binarization of the corneal profile [87].

In contrast to ORA, which measures applanations from the detected signal, the Corvis ST analyses a structural image. On its basis, the Corvis ST provides information about the applanation time (A1T, A2T), length (A1L, A2L), and corneal deformation velocity (A1V, A2V) (Figure 5) [4, 19, 80, 82]. The other parameter is the highest concavity (HC), which is measured when the cornea achieves its maximum concavity during the air puff (Figure 5). The highest concavity time (HCT) and the highest concavity deformation amplitude (HCDA) can be assessed (Figure 5) [4, 81, 82]. In the Corvis ST, most of the parameters describing the DCR are expressed by time (T) – ms, velocity (V) – m/s and length (L) – mm [4, 80, 81]. The device allows to evaluate the

distance between the two peaks of the cornea during the applanation, i.e. the highest concavity peak distance (HCPD) as well as the highest concavity radius (HCR) [4, 82].

The Corvis ST combined with a Pentacam corneal tomograph provides both biomechanical and tomographic assessment (ARV – Ambrosio, Roberts and Vinciguerra) of the cornea (Figure 6A). The result shows the Corvis Biomechanical Index (CBI), tomographic biomechanical index (TBI) and the tomographic maps of the cornea: curvature and thickness. In turn, the Vinciguerra screening report allows comparing the patient's result with the normative group A (Figure 6B). Additionally, the Ambrosio relational thickness horizontal (ARTh), stiffness parameter at first applanation (SP A1) and corneal biomechanical index (CBI) can be evaluated [4, 82]. Additional parameters form the Corvis ST allow for a comprehensive assessment of the cornea and enable the detection of abnormalities such as KC and PMD at a very early stage, which would not be possible with traditional methods. Analysis of those parameters demonstrates an enhanced screening potential before keratorefractive surgery [88].

In the case of KC, the A1T is lower and A2T is higher than in the normal eyes. In turn, the A1V is higher and A2V is lower in keratoconic eyes than in the normal eyes. The HCDA is higher and the HCR is lower in the KC [89]. After CXL treatment, an increase in the corneal stiffness and significant increase in the A2L and decrease in A2V can be observed [90].

Additionally, in the primary open-angle glaucoma (POAG), a significant longer A2T, lower deformation amplitude and longer peak distance can be observed [91].

Table 2 shows the comparison between the ORA and Corvis ST, as well as the advantages and limitations of each device.

4.3 Air-puff optical coherence elastography

Optical coherence tomography (OCT) is a noninvasive, noncontact, high-speed imaging modality commonly used as a standard tool for ophthalmic diagnosis. OCT acquires information on the light back-scattered from the sample, and translates it into two- or three-dimensional

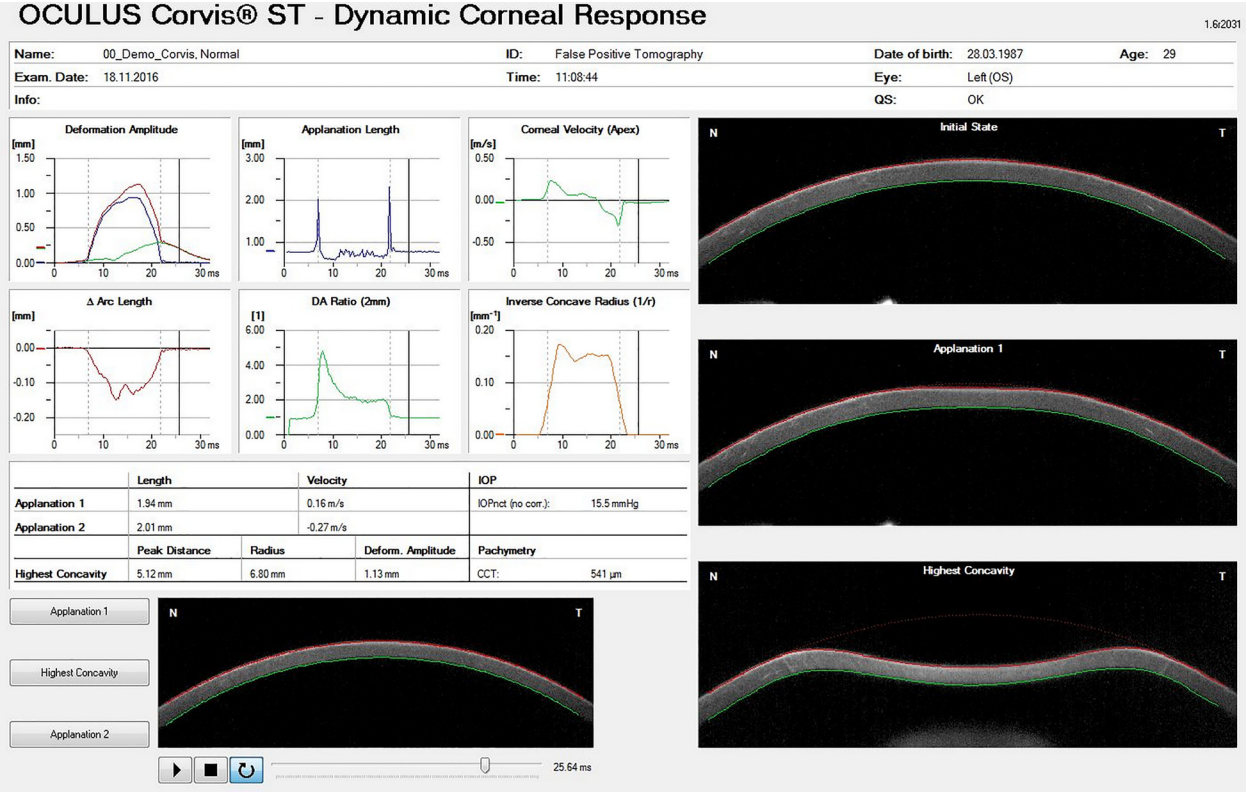

Figure 5: Example of the dynamic corneal response from the Corvis ST in the normal eye: the deformation amplitude, applanation length, inward and outward corneal velocity, and the parameters of the highest concavity (adopted from the Oculus Poland).

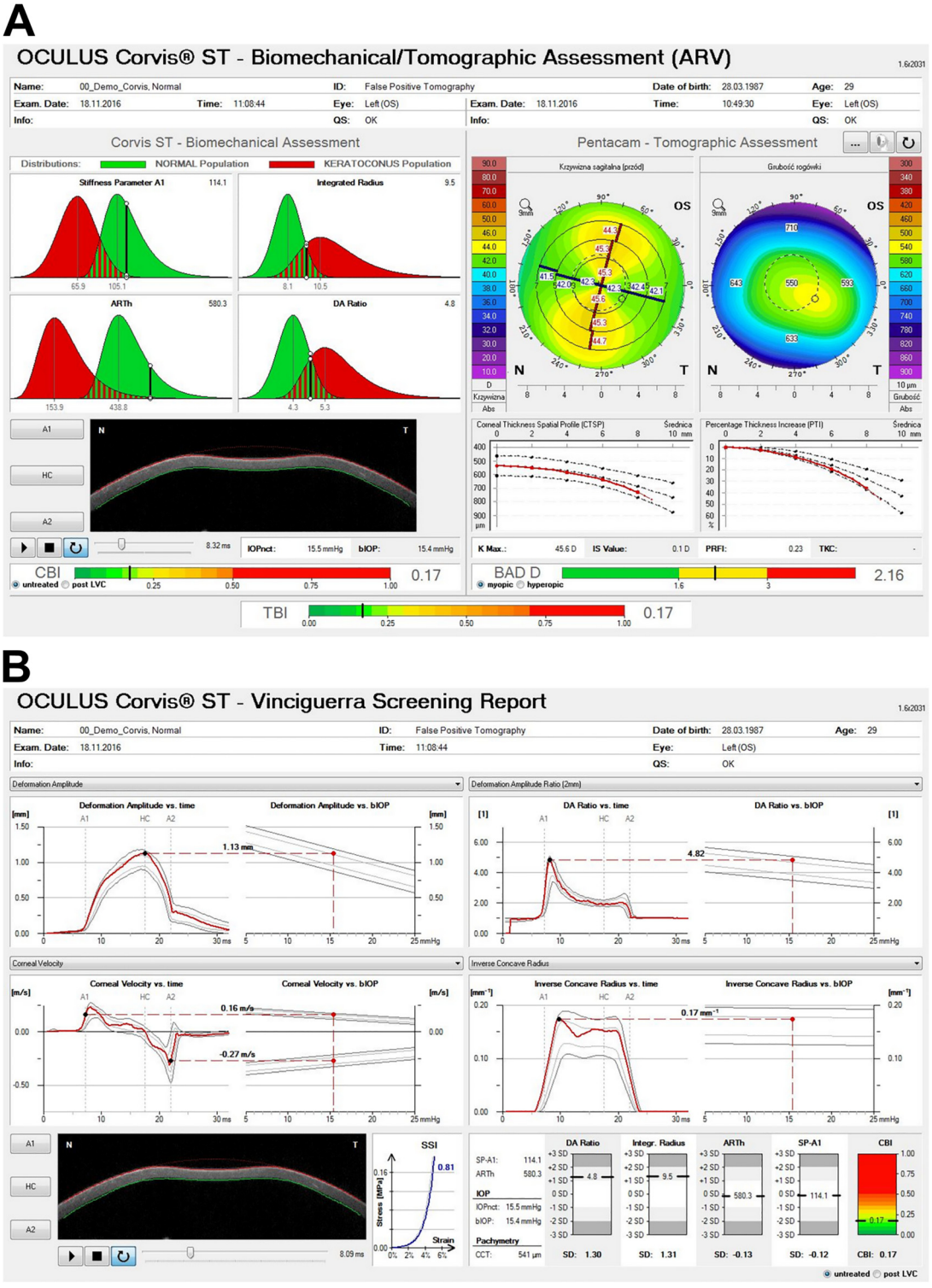

Figure 6: The Corvis ST with Pentacam result in the normal eye. A. The biomechanical and tomographic assessment (ARV) of the cornea with CBI, BAD D, and TBI parameters. B. The Vinciguerra screening report: graphs of deformation amplitude, deformation amplitude ratio, corneal velocity and inverse concave radius dependence on time and bIOP (adopted from the Oculus Poland).

Table 2: Comparison of the most important elements between the ORA and Corvis ST.

	Ocular Response Analyzer	Corvis ST
Application	Assessment of the viscoelastic properties of the cornea and IOP	Assessment of the dynamic corneal response and IOP
Stimulus	Air stream	
Principle/aim	Recording of applanation signal with air puff pressure during excitation	Recording a corneal geometry change during air-puff excitation
Subject of analyzes	Applanation signal from corneal apex, pressure of the air puff	Cross-sectional images of the cornea
Most important parameters	CH, CRF, CCF, IOPg, IOPcc	A1T, A2T, A1L, A2L, A1V, A2V, HC, HCDA, HCT, HCPD, HCR
Advantages	Noncontact measurement method	
	– Corneal compensated IOP (IOPcc) and Goldmann correlated IOP (IOPg) measurement – Assessment the keratoconus match probabilities	– Direct analysis of the dynamic corneal response – Slow-motion video of the corneal deformation with the ability to analyze individual frames – Detailed analysis of the whole eye motion – Measurement of the thickness of the cornea – Biomechanical corrected IOP (bIOP) measurement – Possibility of biomechanical and tomographic evaluation of the cornea at the same time
	– Measurement of the mechanical response of the cornea not directly related to Young's modulus – No assessment of spatial differences in the properties of the cornea across the width and depth (influence extracorneal structures)	
Limitations	– Does not provide information about energy dissipation – Indirect analysis of the corneal response based on the signal from detector – Measurement based on the behavior of only the apex of the cornea – Information about eye movement in not available	– Incomplete analysis of the whole eye movement – Only horizontal meridian of cornea is measured

image of the internal structure of the sample with micrometer resolution [92–94]. The elastographic extension of OCT enables to image tissue displacement during perturbation (loading) [53, 95]. Although OCT-based elastography (OCE) was first demonstrated in 1998 [54], the main breakthrough in imaging of ocular elasticity came with development Fourier-domain detection [92]. New generation of the OCT systems (Fourier/spectral-domain OCT) enabled ~50–100 times faster imaging, and thus much reduction motion artefacts. The sensitivity was around ~20 dB higher compared to previous instruments with time-domain detection [96–99]. The air-puff stimulus can be applied with OCT system in a number of scenarios to induce perturbation of corneal tissue.

One idea to utilize OCT technology to measure corneal biomechanics is based on combination OCT system together with clinical air puff system.

In noncollinear method described by Dorronsoro et al. [33] two independent instruments: spectral domain OCT system and commercial noncontact tonometer (NT 2000, Hiroishi, Japan) were combined by using tilted mirror (45° in the horizontal direction). The air-puff stimulus generated by tonometer passed through the hole at the center of the mirror; therefore the illuminating beam was provided vertically and reflected towards corneal apex. To avoid overlapping optical axis with the hole and enable proper scanning, additional small tilt (8°) of the mirror was added. In consequence of the noncollinear configuration of the system, direction of air-puff was slightly shifted in relation to the optical axis determined by OCT. The instrument was capable of working in two modes: 1-D configuration enabled to image temporal corneal apex deformation, and 2-D configuration used to image spatial profile during air-puff excitation [33]. The approach was employed to study the effect of IOP, thickness, dehydration state, cross-linking (increasing tissue rigidity) as well as the impact of the sclera and ocular muscles on corneal deformation during air puff test [33, 57].

On the other hand, integration of the OCT instrument with the clinical air puff system can be performed in collinear way as was demonstrated by Alonso-Caneiro et al. [38]. The high speed swept-source OCT (SS-OCT), working at the central wavelength of 1310 nm and speed of 50,000 A-scans per second, was combined with air puff

chamber from commercial noncontact tonometer [XPert NCT; Reichert Inc., Buffalo, NY] to acquire information about corneal apex displacement during excitation. The system enabled to simultaneously acquire series of subsequent A-scans (so called M-scan) at the same position, together with temporal profile of the applied force. Glass window incorporated into the chamber made the optical axis of SS-OCT collinear with the direction of applied air stream. The instrument was used for analysis of corneal apex displacement and its dynamics during air puff on human subject [38] as well as *ex vivo* measurement of the impact of IOP and crosslinking on corneal response on model animal eyes [11]. Additionally, by combining information about corneal apex displacement with temporal profile of applied force captured simultaneously with OCT data during single measurement, changes in the corneal hysteresis area were analyzed [11]. Later, the optical design was improved by combining air-puff chamber with long-range SS-OCT system operating at central wavelength of 1060 nm and at 30 kHz scan rate (Axsun Technologies, Inc., Billerica, MA, USA). Therefore, the movement of the all optical components of the eye and retina along the entire axial eye length under air-puff conditions were observed (Figure 7) [37, 56].

The axial scan rate of the proposed system was ~10 times higher than offers by Corvis ST (based on Scheimpflug camera), but without possibility of transverse scanning [37, 56]. Fast scan rate in combination with high axial resolution (~12 µm in the tissue) allowed for detailed imaging of the dynamics of the cornea, the crystalline lens, and the retina at the same time and providing information on the whole eye movement under mechanical excitation. In addition, the study revealed the existence of interesting effects from corneal tissue reaction such as corneal deflection, eye retraction and crystalline lens wobbling as a result of air-puff stimulus. Information about eye movement during the measurement was used to correct the displacement of the ocular optical components and to show that the elastic properties seems to dominate during corneal reaction on clinical air puff excitation [37, 56].

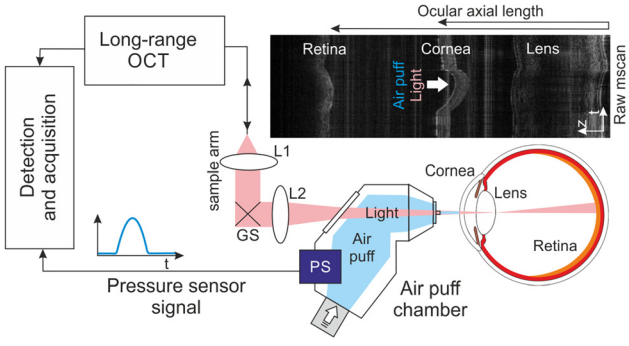

Figure 7: Scheme of the air-puff OCT-based ocular biometry instrument. The system was designed to measure reaction of the all ocular component during air puff action together with the stimulus pressure in time. L1, L2 – lenses, GS – galvo scanners, PS – pressure sensor.

In 2020, Curatelo et al. [58] showed the prototype instrument coupled with air puff unit dedicated for evaluation multimeridian corneal deformation profiles during air-puff event to improve KC detection. The OCT system based on Mach–Zehnder interferometer and operating with VCSEL (MEMS-based vertical-cavity surface emitting laser) swept laser source (SL132120, Thorlabs, USA) at the central wavelength of 1310 nm and speed of 200,000 A-scans per second was coupled with air-puff unit (NT 2000, Nidek Co., Japan) in a collinear way. The idea behind the measuring multiple meridians was based on using very low coil impedance galvo-scanners to apply two scanning patterns (cross-meridian and three horizontal planes) over 15 mm with 1 kHz pattern repetition frequency. Although the instrument showed significantly lower spatial and temporal resolution compared to Corvis ST, the sensitivity was sufficient to detect deformation asymmetry during measurement [58]. Therefore, the proposed approach gives the possibility to identify the softer parts of cornea beyond the apex, which seems to be especially valuable in eccentric KC detection and overcomes limitation of Corvis ST where only horizontal meridian is measured [45, 58, 80, 81, 84].

As mentioned before, standard air puff used in clinical applications as well as in the prototype instruments causes relatively large, millimeter-scale deformation together with whole eye globe movement [37]. Another, much more subtle approach to evaluate corneal biomechanics, is represented by phase-sensitive optical coherence elastography that uses the phase information from interferometric signal. To translate phase signal into displacement, the following formula is used:

$$x(t) = \frac{\lambda \cdot \varphi(t)}{4\pi n}, \tag{13}$$

where x is the displacement, λ is the central wavelength of light source used in OCT system, n is the refractive index of the tissue, and φ is a phase change [32, 62].

The phase analysis of OCT signal increases the sensitivity of the system to detect very low displacements of the cornea, therefore it enables nanometer-range amplitude displacement detection and makes it possible to reduce the level of applied force of stimulus reduction. Focused air puff generates elastic waves that spread perpendicularly to the direction of stimulus [43]. Properties of elastic waves (velocity, time of propagation, relaxation rate) was used in evaluation the mechanical properties of *ex vivo* corneas in

dependency on age [42, 43], thickness [59], IOP [60], corneal depth [36], before and after crosslinking treatment [61]. Next, to measure corneas *in vivo*, the approach was improved by modification air-puff and detection subsystems. The stimulus has been tilted from oblique to perpendicular direction with respect to the tissue surface. In addition, replacing typical reference arm with common light path for sample and reference plane, the same dispersion and polarization was achieved, which improved phase stability of the system and therefore provide higher displacement detection sensitivity [62]. The instrument was used to measure elastic waves velocity in human eyes *in vivo* (2.4–4.2 m/s) as a function of IOP and thickness (both positive correlation) [63]. In a separate project, the natural frequency and damping ratio of the cornea were assessed. Validation of the method on the tissue phantom showed that dominant natural frequency was constant for various pressures of using air and distances between excitation point and point of displacement measuring, but decreased with increasing sample thickness [32]. The next study performed on 20 health human eyes *in vivo* estimated the corneal natural frequency on 234–277 Hz [64].

5 Conclusions

Nowadays, the clinical applications of methodologies enabling assessment of corneal biomechanical properties have increased significantly especially in the detection of ectatic corneal disease and diagnosis of glaucoma. Therefore, one can notice the continuous improvement of the existing methods and the development of new technologies for the assessment of the biomechanical properties of the cornea. The only commercially available devices are ORA and Corvis ST. However, due to limitations and the possibility of obtaining only information about the dynamic response of the cornea, intensive research is currently performed on the optical methods for the assessment of biomechanical properties, including optical coherence elastography.

Author contributions: Conceptualization: P.M., E.M.-W., B.J.K.; analysis of the literature: P.M., E.M.-W. J.R.-Z., I.G. and B.J.K.; writing, original draft preparation: P.M., E.M.-W., J.R.-Z.; P.M., E.M.-W., J.R.-Z.; writing, review and editing: P.M., E.M.-W., J.R.-Z., I.G. and B.J.K.

Research funding: National Science Center, Poland (#2018/31/B/NZ5/02156).

Conflict of interest statement: The authors declare no conflicts of interest regarding this article.

References

[1] W. B. Trattler, P. A. Majmudar, J. I. Luchs, and T. S. Swartz, *Cornea Handbook*, USA, SLACK Incorporated, 2010, pp. 1–12.
[2] M. S. Sridhar, "Anatomy of cornea and ocular surface," *Indian J. Ophthalmol.*, vol. 66, p. 190, 2018.
[3] B. J. Blackburn, M. W. Jenkins, A. M. Rollins, and W. J. Dupps, "A review of structural and biomechanical changes in the cornea in aging, disease, and photochemical crosslinking," *Front. Bioeng. Biotechnol.*, vol. 7, p. 1, 2019.
[4] L. P. G. Escporcatte, M. Q. Salomao, B. T. Lopes, et al., "Biomechanical diagnostics of the cornea," *Eye Vis.*, vol. 7, p. 1, 2020.
[5] A. Kotecha, "What biomechanical properties of the cornea are relevant for the clinician?" *Surv. Ophthalmol.*, vol. 52, p. S109, 2007.
[6] C. J. Roberts, W. J. Dupps, and J. Crawford Downs, *Biomechanics of the Eye*, The Netherlands, Kugler Publications, 2018, pp. 1–522.
[7] S. Kling and F. Hafezi, "Corneal biomechanics – a review," *Ophthalmic Physiol. Opt.*, vol. 37, p. 240, 2017.
[8] N. Garcia-Porta, P. Fernandes, A. Queiros, et al., "Corneal biomechanical properties in different ocular conditions and new measurement techniques," *ISRN Ophthalmol.*, vol. 4, p. 1, 2014.
[9] D. Huang, Y. Huang, Y. Xiao, et al., "Viscoelasticity in natural tissues and engineered scaffolds for tissue reconstruction," *Acta Biomater.*, vol. 97, p. 74, 2019.
[10] D. P. Pinero and N. Alcon, "Corneal biomechanics: a review," *Clin. Exp. Optom.*, vol. 98, p. 1, 2014.
[11] E. Maczynska, K. Karnowski, K. Szulzycki, et al., "Assessment of the influence of viscoelasticity of cornea in animal *ex vivo* model using air-puff optical coherence tomography and corneal hysteresis," *J. Biophotonics*, vol. 12, p. 1, 2019.
[12] J. Ma, Y. Wang, P. Wei, and V. Jhanji, "Biomechanics and structure of the cornea: implications and association with corneal disorders," *Surv. Ophthalmol.*, vol. 63, p. 851, 2018.
[13] N. Terai, F. Raiskup, M. Haustein, L. E. Pillunat, and E. Spoerl, "Identification of biomechanical properties of the cornea: the ocular response analyzer," *Curr. Eye Res.*, vol. 37, p. 553, 2012.
[14] M. Dubbelman, V. A. D. P. Sicam, and G. L. Van der Heijde, "The shape of the anterior and posterior surface of the aging human cornea," *Vis. Res.*, vol. 46, p. 993, 2006.
[15] K. M. Meek and C. Knupp, "Corneal structure and transparency," *Prog. Retin. Eye Res.*, vol. 49, p. 1, 2015.
[16] H. Hatami-Marbini and E. Etebu, "Hydration dependent biomechanical properties of the corneal stroma," *Exp. Eye Res.*, vol. 116, p. 47, 2013.
[17] L. Levin, S. Nilsson, J. Ver Hoeve, S. Wu, and P. Kaufman, *Adler's Physiology of the Eye*, 11th ed. Scotland, Saunders, 2011, pp. 1–808.
[18] K. Wang and B. K. Pierscionek, "Biomechanics of the human lens and accommodative system: functional relevance to physiological states," *Prog. Retin. Eye Res.*, vol. 71, p. 114, 2019.
[19] H. R. Vellara and D. V. Patel, "Biomechanical properties of the keratoconic cornea: a review," *Clin. Exp. Optom.*, vol. 98, p. 31, 2015.
[20] G. Zhang, "Evaluating the viscoelastic properties of biological tissues in a new way," *J. Musculoskelet. Neuronal Interact.*, vol. 5, p. 85, 2005.

[21] N. Sasaki, "*Viscoelasticity - From Theory to Biological Applications*," in *Viscoelastic Properties of Biological Materials*, England, InTech, 2012, pp. 99–122.
[22] T. Glozman and H. Azhari, "A method for characterization of tissue elastic properties combining ultrasonic computed tomography with elastography," *J. Ultrasound Med.*, vol. 29, p. 397, 2010.
[23] C. F. Guimarães, L. Gasperini, A. P. Marques, and R. L. Reis, "The stiffness of living tissues and its implications for tissue engineering," *Nat. Rev. Mater.*, vol. 5, p. 351, 2020.
[24] M. A. Kirby, I. Pelivanov, S. Song, et al., "Optical coherence elastography in ophthalmology," *J. Biomed. Opt.*, vol. 22, p. 1, 2017.
[25] S. J. Petsche, D. Chernyak, J. Maritz, M. E. Levenston, and P. M. Pinksy, "Depth-dependent transverse shear properties of the human corneal stroma," *Invest. Ophthalmol. Vis. Sci.*, vol. 53, p. 873, 2012.
[26] F. A. Duck, *Mechanical Properties of Tissue in: Duck, F.A. Physical Properties of Tissues. A Comprehensive Reference*, England, Academic Press, 1990, pp. 137–165, https://doi.org/10.1016/b978-0-12-222800-1.50009-7.
[27] A. Elsheikh and K. Anderson, "Comparative study of corneal strip extensometry and inflation tests," *J. Roy. Soc. Interface.*, vol. 2, p. 177, 2005.
[28] J. Dias and N. M. Ziebarth, "Impact of hydration media on *ex vivo* corneal elasticity measurements," *Eye Contact Lens*, vol. 41, p. 281, 2015.
[29] K. V. Larin and D. D. Sampson, "Optical coherence elastography – OCT at work in tissue biomechanics [Invited]," *Biomed. Opt. Express*, vol. 8, p. 1172, 2017.
[30] C. Li, G. Guan, Z. Huang, M. Johnstone, and R. K. Wang, "Noncontact all-optical measurement of corneal elasticity," *Opt. Lett.*, vol. 37, p. 1625, 2012.
[31] M. R. Ford, A. S. Roy, A. M. Rollins, and W. J. Dupps, Jr., "Serial biomechanical comparison of edematous, normal, and collagen crosslinked human donor corneas using optical coherence tomography," *J. Cataract Refract. Surg.*, vol. 40, p. 1041, 2014.
[32] G. Lan, K. V. Larin, S. Aglyamov, and M. D. Twa, "Characterization of natural frequencies from nanoscale tissue oscillations using dynamic optical coherence elastography," *Biomed. Opt. Express.*, vol. 11, p. 3301, 2020.
[33] C. Dorronsoro, D. Pascual, P. Pérez-Merino, S. Kling, and S. Marcos, "Dynamic OCT measurement of corneal deformation by an air puff in normal and cross-linked corneas," *Biomed. Opt. Express*, vol. 3, p. 473, 2012.
[34] Ł. Ambroziński, S. Song, S. J. Yoon, et al., "Acoustic micro-tapping for non-contact 4D imaging of tissue elasticity," *Sci. Rep.*, vol. 6, p. 1, 2016.
[35] B. I. Akca, E. W. Chang, S. Kling, et al., "Observation of sound-induced corneal vibrational modes by optical coherence tomography," *Biomed. Opt. Express*, vol. 6, p. 3313, 2015.
[36] S. Wang and K. V. Larin, "Noncontact depth-resolved micro-scale optical coherence elastography of the cornea," *Biomed. Opt. Express*, vol. 5, p. 3807, 2014.
[37] E. Maczynska, J. Rzeszewska-Zamiara, A. Jimenez Villar, et al., "Air-puff-induced dynamics of ocular components measured with optical biometry," *Invest. Ophthalmol. Vis. Sci.*, vol. 60, p. 1979, 2019.
[38] D. Alonso-Caneiro, K. Karnowski, B. J. Kaluzny, A. Kowalczyk, and M. Wojtkowski, "Assessment of corneal dynamics with high-speed swept source optical coherence tomography combined with an air puff system," *Opt. Express*, vol. 19, p. 14188, 2011.
[39] C. S. Johnson, S. I. Mian, S. Moroi, et al., "Role of corneal elasticity in damping of intraocular pressure," *Invest. Ophthalmol. Vis. Sci.*, vol. 48, p. 2540, 2007.
[40] M. Singh, J. Li, Z. Han, et al., "Assessing the effects of riboflavin/UV-A crosslinking on porcine corneal mechanical anisotropy with optical coherence tomography," *Biomed. Opt. Express*, vol. 8, p. 349, 2017.
[41] D. V. Litwiller, S. J. Lee, A. Kolipaka, et al., "MR elastography of the *ex vivo* bovine globe," *J. Magn. Reson. Imag.*, vol. 32, p. 44, 2010.
[42] J. Li, S. Wang, M. Singh, et al., "Air-pulse OCE for assessment of age-related changes in mouse cornea *in vivo*," *Laser Phys. Lett.*, vol. 11, p. 065601, 2014.
[43] S. Wang and K. V. Larin, "Shear wave imaging optical coherence tomography (SWI-OCT) for ocular tissue biomechanics," *Opt. Lett.*, vol. 39, p. 41, 2014.
[44] Y. K. Mariappan, K. J. Glaser, and R. L. Ekhman, "Magnetic resonance elastography: a review," *Clin. Anat.*, vol. 23, p. 497, 2011.
[45] D. P. Piñero and N. Alcón, "*In vivo* characterization of corneal biomechanics," *J. Cataract Surg.*, vol. 40, p. 870, 2014.
[46] K. Clayson, E. Pavlatos, X. Pan, et al., "Ocular pulse elastography: imaging corneal biomechanical responses to stimulated ocular pulse using ultrasound," *Transl. Vis. Sci. Technol.*, vol. 9, p. 1, 2020.
[47] R. Muthupillai, D. J. Lomas, P. J. Rossman, et al., "Magnetic resonance elastography by direct visualization of propagating acoustic strain waves," *Science*, vol. 269, p. 1854, 1995.
[48] G. Scarcelli, R. Pineda, and S. H. Yun, "Brillouin optical microscopy for corneal biomechanics," *Invest. Ophthalmol. Vis. Sci.*, vol. 53, p. 185, 2012.
[49] S. Nakakura, Y. Kiuchi, M. Kaneko, et al., "Evaluation of corneal displacement using high-speed photography at the early and late phases of noncontact tonometry," *Invest. Ophthalmol. Vis. Sci.*, vol. 54, p. 2474, 2013.
[50] S. Kling, L. Remon, A. Pérez-Escudero, J. Merayo-Lloves, and S. Marcos, "Corneal biomechanical changes after collagen cross-looking from porcine eye inflation experiments," *Invest. Ophthalmol. Vis. Sci.*, vol. 51, p. 3961, 2010.
[51] C. Liu, A. Schill, C. Wu, M. Singh, and K. V. Larin, "Non-contact single shot elastography using line field low coherence holography," *Biomed. Opt. Express*, vol. 7, p. 3021, 2016.
[52] S. Li, K. D. Mohan, W. W. Sanders, and A. L. Oldenburg, "Toward soft-tissue elastography using digital holography to monitor surface acoustic waves," *J. Biomed. Opt.*, vol. 16, p. 1, 2011.
[53] B. F. Kennedy, K. M. Kennedy, A. L. Oldenburg, et al., "Optical coherence elastography," in *Optical Coherence Tomography – Technology and Applications*, W. Drexler and J. G. Fujimoto, Eds., Germany, Springer, 2015, pp. 1007–1054.
[54] J. Schmitt, "OCT elastography: imaging microscopic deformation and strain of tissue," *Opt. Express*, vol. 3, p. 199, 1998.
[55] J. Hong, J. Xu, A. Wei, et al., "A new tonometer – the Corvis ST tonometer: clinical comparison with non-contact and Goldmann applanation tonometers," *Invest. Ophthalmol. Vis. Sci.*, vol. 54, p. 695, 2013.
[56] A. Jimenez-Villar, E. Mączyńska, A. Cichański, et al., "High-speed OCT-based ocular biometer combined with air-puff system for

determination of induced retraction-free eye dynamics," *Biomed. Opt. Express*, vol. 10, p. 3663, 2019.
[57] S. Marcos, S. Kling, N. Bekesi, and C. Dorronsoro, "Corneal biomechanical properties from air-puff corneal deformation imaging," *Proc. SPIE*, vol. 8946, p. 894609, 2014.
[58] A. Curatolo, J. S. Birkenfeld, E. Martinez-Enriquez, et al., "Multi-meridian corneal imaging of air-puff induced deformation for improved detection of biomechanical abnormalities," *Biomed. Opt. Express*, vol. 11, p. 6337, 2020.
[59] S. Vantipalli, J. Li, M. Singh, et al., "Effects of thickness on corneal biomechanical properties using optical coherence elastography," *Optom. Vis. Sci.*, vol. 95, p. 299, 2018.
[60] M. Singh, J. Li, Z. Han, et al., "Investigating elastic anisotropy of the porcine cornea as a function of intraocular pressure with optical coherence tomography," *J. Refract. Surg.*, vol. 32, p. 562, 2016.
[61] J. Li, Z. Han, M. Singh, M. D. Twa, and K. V. Larin, "Differentiating untreated and cross-linked porcine corneas of the same measured stiffness with optical coherence elastography," *J. Biomed. Opt.*, vol. 19, p. 110502, 2014.
[62] G. Lan, M. Singh, K. V. Larin, and M. D. Twa, "Common-path phase-sensitive optical coherence tomography provides enhanced phase stability and detection sensitivity for dynamic elastography," *Biomed. Opt. Express*, vol. 8, p. 5253, 2017.
[63] G. Lan, S. R. Aglyamov, K. V. Larin, and M. D. Twa, "In vivo human corneal shear-wave optical coherence elastography," *Optom. Vis. Sci.*, vol. 98, p. 58, 2021.
[64] G. Lan, S. Aglyamov, K. V. Larin, and M. D. Twa, "In vivo human corneal natural frequency quantification using dynamic optical coherence elastography: repeatability and reproducibility," *J. Biomech.*, vol. 121, p. 110427, 2021.
[65] S. Kaushik and S. S. Pandav, "Ocular response analyzer," *J. Curr. Glaucoma Pract.*, vol. 6, p. 17, 2012.
[66] S. M. Sayed and R. K. Lee, "Corneal biomechanical properties and their role in glaucoma diagnosis and management," *Int. Ophthalmol. Clin.*, vol. 58, p. 35, 2018.
[67] H. S. Hwang, S. K. Park, and M. S. Kim, "The biomechanical properties of the cornea and anterior segment properties," *BMC Ophthalmol.*, vol. 49, p. 1, 2013.
[68] S. Franco and M. Lira, "Biomechanical properties of the cornea measured by the Ocular Response Analyzer and their association with intraocular pressure and the central corneal curvature," *Clin. Exp. Optom.*, vol. 92, p. 469, 2009.
[69] A. A. K. E. Massry, A. A. Said, I. M. Osman, et al., "Corneal biomechanics in different age groups," *Int. Ophthalmol.*, vol. 40, p. 967, 2020.
[70] S. Shah, M. Laiquzzaman, R. Bhojwani, S. Mantry, and I. Cunliffe, "Assessment of the biomechanical properties of the cornea with the ocular response analyzer in normal and keratoconic eyes," *Invest. Ophthalmol. Vis. Sci.*, vol. 48, p. 3026, 2007.
[71] F. A. Medeiros, A. Meira-Feritas, R. Lisboa, et al., "Corneal hysteresis as a risk factor for glaucoma progression: a prospective longitudinal study," *Ophthalmology*, vol. 120, p. 1533, 2013.
[72] Y. Hong, N. Shoji, T. Morita, et al., "Comparison of corneal biomechanical properties in normal tension glaucoma patients with different visual field progression speed," *Int. J. Ophthalmol.*, vol. 9, p. 973, 2016.
[73] D. Wu, Y. Wang, L. Zhang, S. Wei, and X. Tang, "Corneal biomechanical effects: small-incision lenticule extraction versus femtosecond laser-assisted laser in situ keratomileusis," *J. Cataract Refract. Surg.*, vol. 40, p. 954, 2014.
[74] H. Hashemi, A. Beiranvand, A. Yekta, A. Asharlous, and M. Khabazkhoob, "Biomechanical properties of early keratoconus: suppressed deformation signal wave," *Contact Lens Anterior Eye*, vol. 40, p. 104, 2017.
[75] G. Labiris, A. Giarmoukakis, Z. Gatzioufas, et al., "Diagnostic capacity of the keratoconus match index and keratoconus match probability in subclinical keratoconus," *J. Cataract Refract. Surg.*, vol. 40, p. 999, 2014.
[76] A. Jóźwik, M. Asejczyk-Widlicka, A. Boszczyk, H. Kasprzak, and P. Krzyżanowska-Berkowska, "Raw data from Ocular Response Analyzer applied for differentiation of normal and glaucoma patients," *Opt. Appl.*, vol. 50, p. 147, 2020.
[77] S. Zarei-Ghanavati, A. Ramirez-Miranda, F. Yu, and D. R. Hamilton, "Corneal deformation signal waveform analysis in keratoconic versus post-femtosecond laser in situ keratomileusis eyes after statistical correction for potentially confounding factors," *J. Cataract Refract. Surg.*, vol. 38, p. 607, 2012.
[78] S. Asano, R. Asaoka, T. Yamashita, et al., "Visualizing the dynamic change of Ocular Response Analyzer waveform using Variational Autoencoder in association with the peripapillary retinal arteries angle," *Sci. Rep.*, vol. 10, p. 6592, 2020.
[79] A. Luz, B. Lopes, K. M. Hallahan, et al., "Discriminant value of custom ocular response analyzer waveform derivatives in forme fruste keratoconus," *Am. J. Ophthalmol.*, vol. 164, p. 14, 2016.
[80] H. Lee, D. S. Y. Kang, B. J. Ha, et al., "Biomechanical properties of the cornea using a dynamic Scheimpflug analyzer in healthy eyes," *Yonsei Med. J.*, vol. 59, p. 1115, 2018.
[81] R. Ambrósio, Jr., I. Ramos, A. Luz, et al., "Dynamic ultra-high speed Scheimpflug imaging for assessing corneal biomechanical properties," *Rev. Bras. Ophthalmol.*, vol. 72, p. 99, 2013.
[82] K. Yang, L. Xu, Q. Fan, D. Zhao, and S. Ren, "Repeatability and comparison of new Corvis ST parameters in normal and keratoconus eyes," *Sci. Rep.*, vol. 9, p. 15379, 2019.
[83] C. J. Roberts, "Importance of accurately assessing biomechanics of the cornea," *Curr. Opin. Ophthalmol.*, vol. 27, p. 285, 2016.
[84] X. Chen, A. Stojanovic, Y. Hua, et al., "Reliability of corneal dynamic Scheimpflug analyser measurements in virgin and post-PRK eyes," *PLoS One*, vol. 9, p. e1109577, 2014.
[85] M. Jędzierowska, "Corvis ST tonometer and the possibility of analysing corneal deforamtion dynamics during intraocular pressure measurement," in *Air-Puff Tonometers: Challenges and Insights*, R. Koprowski, Ed., England, Institute of Physics Publishing Ltd, 2019, pp. 1–13.
[86] H. Kasprzak and A. Boszczyk, "Numerical analysis of corneal curvature dynamics based on Corvis tonometer images," *J. Biophotonics*, vol. 9, p. 436, 2016.
[87] M. Jędzierowska, R. Koprowski, S. Wilczyński, and K. Krysik, "A new method for detecting the outer corneal contour in images from an ultra-fast Scheimpflug camera," *Biomed. Eng. Online.*, vol. 18, p. 115, 2019.
[88] V. Silbiger De Stefano and W. J. Dupps, Jr., "Biomechanical diagnostics of the cornea," *Int. Ophthalmol. Clin.*, vol. 57, p. 75, 2017.
[89] R. Elham, E. Jafarzadehpur, H. Hashemi, et al., "Keratoconus diagnosis using Corvis ST measured biomechanical parameters," *J. Curr. Ophthalmol.*, vol. 29, p. 175, 2017.

[90] R. Salouti, M. R. Khalili, M. Zamani, M. Ghoreyshi, and M. H. Nowroozzadeh, "Assessment of the changes in corneal biomechanical properties after collagen cross-linking in patients with keratoconus," *J. Curr. Ophthalmol.*, vol. 31, p. 262, 2019.
[91] L. Tian, D. Wang, Y. Wu, et al., "Corneal biomechanical characteristics measured by the Corvis Scheimpflug technology in eyes with primary open-angle glaucoma and normal eyes," *Acta Ophthalmol.*, vol. 34, p. e317, 2016.
[92] A. F. Fercher, C. K. Hitzenberger, G. Kamp, and S. Y. El-Zaiat, "Measurement of intraocular distances by backscattering spectral interferometry," *Opt. Commun.*, vol. 117, p. 43, 1995.
[93] J. F. de Boer, R. Leitgeb, and M. Wojtkowski, "Twenty-five years of optical coherence tomography: the paradigm shift in sensitivity and speed provided by Fourier domain OCT [Invited]," *Biomed. Opt. Express*, vol. 8, p. 3248, 2017.
[94] D. Huang, E. A. Swanson, C. P. Lin, et al., "Optical coherence tomography," *Science*, vol. 254, p. 1178, 1991.
[95] J. Chong and W. J. Dupps, Jr., "Corneal biomechanics: measurement and structural correlations," *Exp. Eye Res.*, vol. 205, p. 1, 2021.
[96] M. Wojtkowski, R. Leitgeb, A. Kowalczyk, T. Bajraszewski, and A. F. Fercher, "In vivo human retinal imaging by Fourier domain optical coherence tomography," *J. Biomed. Opt.*, vol. 7, p. 457, 2002.
[97] M. A. Choma, M. V. Sarunic, C. Yang, and J. Izatt, "Sensitivity advantage of swept source and Fourier domain optical coherence tomography," *Opt. Express*, vol. 11, p. 2183, 2003.
[98] J. F. de Boer, B. Cense, B. H. Park, M. C. Pierce, G. J. Tearney, and B. E. Bouma, "Improved signal-to-noise ratio in spectral-domain compared with time-domain optical coherence tomography," *Opt. Lett.*, vol. 28, p. 2067, 2003.
[99] R. Leitgeb, C. Hitzenberger, and A. F. Fercher, "Performance of Fourier domain vs. time domain optical coherence tomography," *Opt. Express*, vol. 11, p. 889, 2003.

Bionotes

Patryk Mlyniuk (b.1995) obtained a MSc in Optometry at the Collegium Medicum in Bydgoszcz Nicolaus Copernicus University in Torun (Poland) in 2019. After obtaining a master's degree, he began studies at the Doctoral School of Medical and Health Sciences at the Nicolaus Copernicus University in Torun. The subject of his PhD thesis is *Assessment of the biomechanical properties of the anterior segment in eyes with keratoconus*. The main research interests concern issues in the field of optometry and ophthalmology, including contactology and aspects related to the anterior segment of the eye. In cooperation with the Institute of Physics of the Nicolaus Copernicus University in Torun (Poland), he participates in research on other applications of optical coherence tomography (OCT). He is an author or coauthor of scientific papers, conference presentations and scientific posters. The most important publications of the author include: 1) Kałużny Bartłomiej J., Stachura Joanna, Młyniuk Patryk, Jimenez-Villar Alfonso, Wietlicka-Piszcz Magdalena, Grulkowski Ireneusz. *Change in the geometry of positive- and negative-powered soft contact lenses during wear.* PLoS ONE, 2020, vol. 15, pp. 1–12. 2) Stachura Joanna, Młyniuk Patryk, Błoch Waldemar, Jimenez-Villar Alfonso, Grulkowski Ireneusz, Kałużny Bartłomiej J. *Shape of the anterior surface of the cornea after extended wear of silicone hydrogel soft contact lenses.* Ophthalmic and Physiological Optics, 2021, vol. 41 (4), pp. 683–690. 3) Młyniuk Patryk, Stachura Joanna, Jimenez-Villar Alfonso, Grulkowski Ireneusz, Kałużny Bartłomiej J. *Changes in the geometry of modern daily disposable soft contact lenses during wear.* Scientific Reports, 2021, vol. 11, pp. 1–8.

Ewa Maczynska-Walkowiak (b.1989) received her MSc in Medical Biotechnology from the Nicolaus Copernicus University (NCU) in Toruń (Poland) in 2014. Currently, she is a PhD student in Bio-Optics & Optical Engineering Lab (BOEL) at NCU in Toruń. Her main research interest include developing optical imagine tools for ophthalmology applications. Mączyńska-Walkowiak is experience in physics, biomedicine and optics engineering. She is especially focus on development advanced optical coherence tomography instruments for ocular structure biomechanics investigation.

Jagoda Rzeszewska-Zamiara graduated the Faculty of Medicine of the Medical Academy in Bydgoszcz Poland in 2012. In 2021 she finished specialization in ophthalmology. She is PhD student in Nicolaus Copernicus University in Torun (Poland). Her professional interests includes OCT, cornea, keratoconus, keratorefractive surgery, eyelid surgery. Being an employee of Ophthalmology and Optometry at Collegium Medicum NCU, she is a teacher of medicine and optometry students. Main publication: 1) Kaluzny Bartlomiej J., Verma S.,

Piotrowiak-Slupska Ilona, Kaszuba-Modrzejewska Magdalena, Rzeszewska-Zamiara Jagoda, Stachura Joanna, Arba-Mosquera S. “Three-year outcomes of mixed astigmatism correction with single-step transepithelial photorefractive keratectomy with a large ablation zone”J. Cataract Refract. Surg.2021: Vol. 47, nr 4, s. 450–458. 2) Stachura Joanna, Seredyka-Burduk Malgorzata, Piotrowiak-Slupska Ilona, Kaszuba-Modrzejewska Magdalena, Rzeszewska-Zamiara Jagoda, Kalużny Bartlomiej J. “Developments in contact lens imaging: new applications of optical coherence tomography”Appl. Sci.-Basel 2019: Vol. 9, nr 13, s. 2580, 1–13. 3) Mączynska E., Rzeszewska-Zamiara Jagoda, Jimenez Villar A., Wojtkowski M., Kaluzny Bartlomiej J., Grulkowski I. “Air-puff-induced dynamics of ocular components measured with optical biometry” Investig. Ophthalmol. Vis. Sci. 2019: Vol. 60, nr 6, s. 1979–1986.

Ireneusz Grulkowski (b. 1979) received his MSc in Biomedical Physics from the University of Gdańsk (Poland) in 2003. Two years later, Grulkowski graduated also from Intercollegiate Faculty of Biotechnology of the University of Gdańsk and Medical University of Gdańsk (Biotechnology). Ireneusz Grulkowski received PhD in Experimental Physics from the University of Gdańsk based on the thesis entitled ‘Diffraction of light by cylindrical ultrasound’. Later on, he worked as an assistant professor at the University of Gdańsk and at the Nicolaus Copernicus University (NCU, Torun, Poland), where he joined Medical Physics Group (leader: Prof. Maciej Wojtkowski). At that time, his research was devoted to novel applications of optical coherence tomography (OCT). In 2010–2012, Dr. Grulkowski was a Postdoctoral Research Associate (Visiting Scientist) at Massachusetts Institute of Technology (Cambridge, USA) under the supervision of Prof. James G. Fujimoto. He developed new long-range eye imaging applications with Swept Source OCT with the vertical cavity surface emitting laser. Dr. Grulkowski obtained habilitation in December 2016, and launched Bio-Optics & Optical Engineering Lab (BOEL) at NCU in 2017. Dr. Grulkowski has been appointed Associate Professor at NCU in October 2018. The scientific interests of BOEL cover application of advanced optical engineering methods in biomedical imaging as well as studies of optical and biomechanical properties of ocular structures. Grulkowski group collaborates with many research centers in Poland and abroad. His publication record includes 71 publications and 4 book chapters that were cited over 1000 times in total. Prof. Grulkowski presented his work at many domestic and international conferences and workshops (>100 presentations, incl. 13 invited talks). His research has been funded by: Foundation for Polish Science, Polish National Science Center, Polish Ministry of Science and Higher Education, European Fund for Regional Development etc.

Bartlomiej J. Kaluzny graduated the Faculty of Medicine of the Medical Academy in Bydgoszcz Poland in 1999. In 2005 he received a PhD diploma and in 2006 he finished specialization in ophthalmology. Since 2005 he had been a member of research team which constructed and performed clinical trials of first Spectral domain OCT prototype (SOCT). He was responsible for investigation of SOCT applications in anterior segment of the eye. His professional interests evolved from OCT to ophthalmic surgery, including cataract and refractive surgery and corneal transplantation. He is an author or co-author of more than 80 scientific papers and a reviewer for professional journals such as Ophthalmology, Cornea and Optometry and Vision Science. Being a Head of Division of Ophthalmology and Optometry at Collegium Medicum NCU, he is a teacher of medicine and optometry students. Part of his career was also devoted to educate and train young ophthalmologists to cataract and refractive surgery.